Data supplement for Ching et al., Mapping Subcortical Brain Alterations in 22q11.2 Deletion Syndrome: Effects of Deletion Size and Convergence With Idiopathic Neuropsychiatric Illness. Am J Psychiatry (doi: 10.1176/appi.ajp.2019.19030284).

Supplemental Methods

CONTENTS

1. Study Participant Ascertainment and Assessment

All cases received a molecularly confirmed diagnosis of 22q11.2 deletion. Microdeletion size was measured from peripheral blood samples using a multiplex ligation-dependent probe amplification (Sørensen 2010). Microdeletion breakpoints tend to occur within four regions of low copy repeats lying within the 22q11.2 region. The most common deletion subtype, found in ~85% of cases, involves the loss of ~3 megabases (Mb) of DNA, and is known as the LCR22A-LCR22D or A-D deletion. A smaller 1.5 Mb deletion, termed the LCR22A-LCR22B or A-B deletion, is the next most common subtype, found in ~10% of cases.

All 22q11DS subjects included in the psychotic disorder group had a DSM schizophrenia spectrum psychotic disorder diagnosis (schizophrenia, schizoaffective disorder, or psychosis not otherwise specified), as determined via structured diagnostic interview conducted by a trained mental health professional at each site, and supplemented by collateral information and medical records. See **Supplemental Table S4** regarding study instruments and study inclusion/exclusion criteria. A cross-site reliability procedure was conducted in which two investigators with clinical expertise independently reviewed a subset of representative cases from each site (Gur 2017). **Supplemental Table S4** references provide detailed information regarding clinical and demographic characteristics of each study sample.

2. Visual Quality Control and Image Exclusions Criteria

All image segmentations and subcortical shape models were examined by the first author (CC) using ENIGMA-standardized visual quality control procedures, which can be found online: http://enigma.ini.usc.edu/protocols/imaging-protocols/.

One 22q11DS subject had large ventricles compared to the rest of the cohort. However, there was no quality control reason to remove this subject from the 22q11DS vs. HC analysis. As larger ventricles appear to be associated with 22q11DS and both the scan and segmentation were of good quality, we kept this particular subject in the 22q11DS vs. HC analysis as they represent our goal of analyzing an ecologically valid 22q11DS cohort. This subject was not included in the deletion subtype and psychosis analyses after subject matching for age and sex.

3. ENIGMA Subcortical Shape Analysis Technique Details

A surface mesh model is created for each ROI FreeSurfer volume (left and right hippocampus, amygdala, caudate, putamen, pallidum, thalamus and nucleus accumbens) and then registered to the ENIGMA shape template using a Medial Demons approach (Gutman 2013). Each structure was computationally represented as a mesh of triangular tiles, where the points on the surface make up vertices that form the overall 3D mesh. A medial model was fit for each structure and was used along with intrinsic shape features to drive registration to the template (Gutman 2015; Gutman 2015a). Two point-wise measures of shape morphometry were derived. The first, termed *radial distance*, is the distance of each vertex to the medial curve and represents a measure of local thickness. At each point $\boldsymbol{p} \in \mathcal{M}$ on the surface, and given a medial curve $\boldsymbol{c}$: $[0,1] \rightarrow \mathbb{R}^3$, the radial distance is defined by

$$D(\boldsymbol{p}) = \min\{\|\boldsymbol{c}(t) - \boldsymbol{p}\| \, | t \in [0,1]\}$$

The second measure, based on surface Tensor Based Morphometry (TBM), generalizes TBM from Euclidean spaces to surfaces (Gutman 2012; Gutman 201a). The differential map between the tangent spaces of two surfaces replaces the Jacobian:

$$J: T\mathcal{M}_t \rightarrow T\mathcal{M}$$

In our model, $\mathcal{M}_t$ was the average template, and $\mathcal{M}$ was the surface we wished to study. J is a linear mapping, and may be thought of as the restriction of the standard Jacobian to the tangent spaces of the template and study surfaces. It is possible to analyze the full tensor using Log-Euclidean metrics on SPD matrices (Wang 2011; Gutman 2015a), but such analyses are difficult to interpret. Instead, our model considers the Jacobian determinant, representing the surface dilation ratio between the template and the study subject. This measure can be interpreted as the areal dilation (stretching and contracting) required to match a small surface patch around a particular point of the template surface to the small patch of area around the corresponding point on the individual subject. A higher Jacobian value suggests larger volume for that specific subregion of the structure. Our final TBM measure was the logarithm of the Jacobian determinant, to obtain a distribution closer to Gaussian.

While subcortical volumes often scale with overall brain size (intracranial volume or ICV) (i.e., a larger overall brain correlates with larger overall subcortical structures), we also fit alternative models for the shape analyses in which the volume of each structure was used as a covariate instead of ICV to identify any regionally selective effects on structures beyond those accounted for by overall volume (see **Supplemental Figures**). A modified searchlight FDR procedure was applied globally across all structures for each statistical model (Langers 2007; Kriegeskorte 2006). The searchlight procedure defined distance as the Euclidean distance between the atlas shape vertices. The distance between vertices of different structures was set to infinity. This particular procedure is more conservative than one that assumes spatial correlation between the boundaries of different structures, though is less conservative than the original FDR procedure that assumes all vertices represent independent statistical tests.

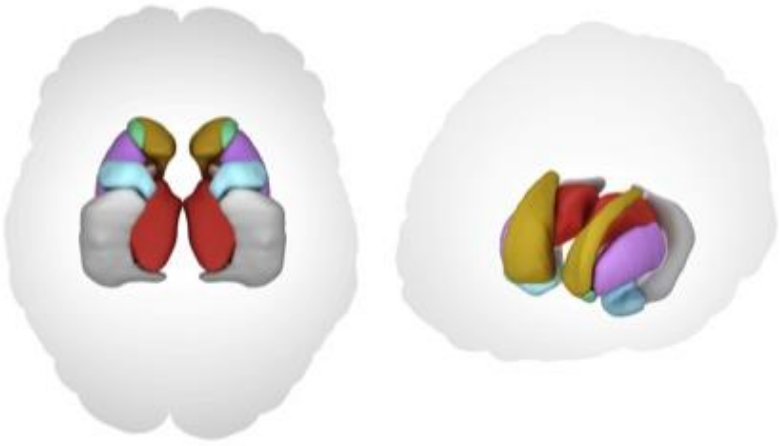

Above are representations of the subcortical surface templates for the 7 structures of interest: left and right nucleus accumbens, amygdala, caudate, hippocampus, putamen, pallidum, and thalamus. The hippocampus lies beneath the 6-layered neocortex. While classified as archicortex, the hippocampus was considered a subcortical structure for these analyses. *Left image: inferior view: right image: anterior/lateral view.*

ROI	Total # of Surface Vertices
Amygdala	1368
Caudate	2502
Hippocampus	2502
Nucleus Accumbens	930
Pallidum	1254
Putamen	2502
Thalamus	2502

Above are the number of vertices sampled from each ROI, with larger structures including a greater number of vertices.

4. Statistical Modeling and Figure Plotting

All multiple linear regression models were fit using R's lm function. Anova model comparisons were run using R's *anova* function. Analysis of covariance (ANCOVA) models were fit using R's *aov* function. All plots were created using *ggplot2*.

5. Medication Effects on Subcortical Structure

Medication use at the time of MRI scan acquisition was grouped into 6 categories: typical (1st generation) antipsychotics (N=14), atypical (2nd generation) antipsychotics (N=63), antidepressants (N=83), and anticonvulsants (mood stabilizers; N=22) (**Supplemental Table S1**)**.** Lithium was excluded as only four subjects had an available record of lithium use at the time of scan. Other psychotropic agents were excluded from the analysis due to high heterogeneity. Using all the available medication data, the effects of the medications on regional cortical measures were modeled using general linear models, including the medication categories as independent variables, while controlling for other confounding factors of site, sex, and age. The results are presented in **Supplemental Table S13**.

6. Statistical Analysis Details: 22q11DS vs. HC

Group differences between the 437 participants with 22q11DS and 330 HC were assessed using multiple linear regression. 22q11DS subjects from the Utrecht and Toronto 2 sites were withheld from this analysis as they lacked matched HC data. The independent variable was group, and

age, age^2, sex, intracranial volume (ICV), and scan site were included as covariates. Follow up analyses included investigations of diagnosis-by-age, diagnosis-by-sex, and medication effects. Additional models treating scanner as a random variable in a linear mixed model approach were also assessed using the *nlme* library in R. Results from the mixed-effects analysis are included in **Supplemental Table S17**. The overall pattern of findings from the mixed-effects models were in line with those results from the fixed effects models.

7. Statistical Analysis Details: Effects of Deletion Size

A comparison of the two most common deletion subtypes (A-D vs. A-B) was carried out on matched samples. Demographic matching provided a cohort of 106 22q11DS subjects with A-D deletions, 23 22q11DS subjects with A-B deletions, and 86 HC (**Supplemental Table S2**). Within site, 22q11DS participants with the A-B deletion were matched with 4-5 subjects with A-D deletions and 4-5 HC of comparable sex and age, as in our study of cortical structure from a highly overlapping sample (Sun 2018). Regional brain volumes were compared across all three groups using an analysis of covariance (ANCOVA), controlling for age, age^2, sex, ICV, and scan site. Multiple linear regressions were fit for all pairwise comparisons of A-D, A-B and HC, adjusting for age, age^2, sex, ICV, and scan site. Follow-up analyses adjusting for medication effects were also conducted.

8. Statistical Analysis Details: Effects of Psychosis

Sixty-four subjects with 22q11DS with a psychotic disorder diagnosis (22q+Psy) were compared to 64 subjects without a history of psychosis (22q-Psy) by matching +/-Psy participants within each site by sex and the nearest possible age (**Supplemental Table S3**). This sample also largely overlapped with the matched sample from our study of cortical brain structure in 22q11DS (Sun 2018). Multiple linear regression models were fit comparing 22q+Psy and 22q-Psy groups, adjusting for age, age^2, sex, ICV, and scan site. Follow-up analyses adjusting for medication effects were also conducted.

9. Cross-Disorder Analysis of Subcortical Effect Sizes

To better compare effect sizes to previously published ENIGMA subcortical studies, as most previously published ENIGMA studies of subcortical volume analyzed averaged left and right volumes, an additional analysis was conducted in which 22q11DS versus HC models were fit on averaged left and right ROI volumes, which again served as the dependent variable, adjusting for age, age^2, sex, ICV and scan site. 22q+Psy versus 22q-Psy averaged ROI models were also fit, adjusting for age, age^2, sex and scan site, excluding ICV, as it was significantly lower in 22q+Psy individuals (see Results).

When fitting 22q11DS versus HC models based on averaged left and right ROI volume, all ROIs were significantly different between groups, and in the same direction as effects from models fit on left and right structures separately (**Supplemental Table S27**). The ROI-averaged model for 22q+Psy versus 22q-Psy also revealed the same pattern of effects to those models fitting left and right ROIs separately, with lower ICV, thalamus, hippocampus and amygdala volumes in 22q+Psy compared to 22q-Psy (**Supplemental Table 28**).

To compare effect sizes, Spearman rank correlations were conducted using R's *ggscatter* function (**Figure 4B)**. Correlograms were created using the R *corrgram* (**Supplemental Figure F10**). All plots were created using *ggplot2*.

ENIGMA studies used in this analysis all performed ENIGMA-harmonized data processing and quality control protocols (available online: http://enigma.ini.usc.edu/protocols/). Adjusted Cohen's *d* effect size estimates and 95% confidence intervals (**Figure 4A**) were taken from the following published studies:

1. **ENIGMA Schizophrenia Working Group (van Erp 2015):** 2028 schizophrenia patients and 2540 healthy controls from 15 sites. Meta-analysis of average left and right volumes adjusting for age, sex, ICV (ICV models adjusted for age and sex).
2. **ENIGMA Major Depression Working Group (Schmaal 2016):** 1728 depression and 7199 healthy controls from 15 sites. Meta-analysis of averaged left and right ROI volumes adjusting for age, sex, ICV.

3. **ENIGMA Bipolar Disorder Working Group (Hibar 2016):** 1710 bipolar patients and 2594 healthy controls from 20 sites. Meta-analysis of averaged left and right volumes adjusting for age, sex, ICV.
4. **ENIGMA Obsessive Compulsive Disorder Group (Boedhoe 2017):** Results taken from the adult analysis (18 or older) included 1495 OCD patients and 1472 healthy controls. Meta-analysis of averaged left and right volumes adjusting for age, sex, ICV.
5. **ENIGMA Autism Spectrum Disorder (van Rooij 2018):** 1571 ASD patients and 1651 health controls from 49 sites. Mega-analysis using mixed model with polynomial effects of age and IQ as well as fixed effects for sex and a random effect for scan site in the main regression model. All subcortical volumes corrected ICV.
6. **ENIGMA Attention Deficit Hyperactivity Disorder (Hoogman 2017):** 1713 ADHD patients and 1529 healthy controls. Mega-analysis linear mixed model adjusting for age, sex, ICV and site as random factor.

References

1. Boedhoe PS, Schmaal L, Abe Y, et al.: Distinct Subcortical Volume Alterations in Pediatric and Adult OCD: A Worldwide Meta- and Mega-Analysis. Am J Psychiatry 2017; 174:60–69

2. van Erp TGM, D P Hibar and, Rasmussen JM, et al.: Subcortical brain volume abnormalities in 2028 individuals with schizophrenia and 2540 healthy controls via the ENIGMA consortium. Molecular Psychiatry 2015; 21:547–553 Available from: https://doi.org/10.1038%2Fmp.2015.63

3. Gur RE, Bassett AS, McDonald-McGinn DM, et al.: A neurogenetic model for the study of schizophrenia spectrum disorders: the International 22q11.2 Deletion Syndrome Brain Behavior Consortium. Mol Psychiatry 2017; 22:1664–1672

4. Gutman BA, Fletcher PT, Cardoso MJ, et al.: A Riemannian Framework for Intrinsic Comparison of Closed Genus-Zero Shapes. Inf Process Med Imaging 2015; 24:205–18

5. Gutman BA, Jahanshad N, Ching CR, et al.: Medial Demons Registration Localizes The Degree of Genetic Influence Over Subcortical Shape Variability: An N= 1480 Meta-Analysis. Proc IEEE Int Symp Biomed Imaging 2015a; 2015:1402–1406

6. Gutman BA, Hua X, Rajagopalan P, et al.: Maximizing power to track Alzheimer's disease and MCI progression by LDA-based weighting of longitudinal ventricular surface features. Neuroimage 2013; 70:386–401

7. Gutman BA, Wang Y, Rajagopalan P, et al.: Shape matching with medial curves and 1-D group-wise registration [Internet], in2012 9th IEEE International Symposium on Biomedical Imaging (ISBI). IEEE, 2012 Available from: https://doi.org/10.1109%2Fisbi.2012.6235648

8. Hibar DP, Westlye LT, van ETG, et al.: Subcortical volumetric abnormalities in bipolar disorder. Mol Psychiatry 2016; 21:1710–1716

9. Hoogman M, Bralten J, Hibar DP, et al.: Subcortical brain volume differences in participants with attention deficit hyperactivity disorder in children and adults: a cross-sectional mega-analysis. Lancet Psychiatry 2017; 4:310–319

10. Kriegeskorte N, Goebel R, Bandettini P: Information-based functional brain mapping. Proceedings of the National Academy of Sciences 2006; 103:3863–3868 Available from: https://doi.org/10.1073%2Fpnas.0600244103

11. Langers DRM, Jansen JFA, Backes WH: Enhanced signal detection in neuroimaging by means of regional control of the global false discovery rate. NeuroImage 2007; 38:43–56Available from: https://doi.org/10.1016%2Fj.neuroimage.2007.07.031

12. van Rooij D, Anagnostou E, Arango C, et al.: Cortical and Subcortical Brain Morphometry Differences Between Patients With Autism Spectrum Disorder and Healthy Individuals Across the Lifespan: Results From the ENIGMA ASD Working Group. Am J Psychiatry 2018; 175:359–369

13. Schmaal L, Veltman DJ, van ETG, et al.: Subcortical brain alterations in major depressive disorder: findings from the ENIGMA Major Depressive Disorder working group. Mol Psychiatry 2016; 21:806–12

14. Sørensen KM, Agergaard P, Olesen C, et al.: Detecting 22q11.2 deletions by use of multiplex ligation-dependent probe amplification on DNA from neonatal dried blood spot samples. J Mol Diagn 2010; 12:147–51

15. Sun D, Ching CRK, Lin A, et al.: Large-scale mapping of cortical alterations in 22q11.2 deletion syndrome: Convergence with idiopathic psychosis and effects of deletion size. Mol Psychiatry 2018;

16. Wang Y, Song Y, Rajagopalan P, et al.: Surface-based TBM boosts power to detect disease effects on the brain: An N=804 ADNI study. NeuroImage 2011; 56:1993–2010 Available from: https://doi.org/10.1016%2Fj.neuroimage.2011.03.040